



HAL
open science

Towards realistic geometric modeling of woven fabrics

Guillaume Couégnat, Hichem Ayadi, Clément Saurat, Eric Rohmer

► **To cite this version:**

Guillaume Couégnat, Hichem Ayadi, Clément Saurat, Eric Rohmer. Towards realistic geometric modeling of woven fabrics. 19th International Conference on Composite Materials (ICCM19), Jul 2013, Montréal, Canada. hal-02341835

HAL Id: hal-02341835

<https://hal.science/hal-02341835>

Submitted on 31 Oct 2019

HAL is a multi-disciplinary open access archive for the deposit and dissemination of scientific research documents, whether they are published or not. The documents may come from teaching and research institutions in France or abroad, or from public or private research centers.

L'archive ouverte pluridisciplinaire **HAL**, est destinée au dépôt et à la diffusion de documents scientifiques de niveau recherche, publiés ou non, émanant des établissements d'enseignement et de recherche français ou étrangers, des laboratoires publics ou privés.

TOWARDS REALISTIC GEOMETRIC MODELING OF WOVEN FABRICS

G. Couégnat*, H. Ayadi, C. Saurat, E. Rohmer
LCTS, CNRS/Univ. Bordeaux/Herakles/CEA, Pessac, France

* Corresponding author (couegnat@lcts.u-bordeaux1.fr)

Keywords: *woven fabric; geometric modeling; textile composite*

1 Introduction

There is a growing interest in the use of textile reinforcements for advanced composite applications [1]. Meso-scale finite element (FE) modeling of woven composite offers a powerful tool to understand the behavior of such materials and to study the effect of their reinforcement architecture on their effective properties [2]. However, the reliability of these approaches is influenced by the way the fabric geometry is approximated. Yarn geometry has only a modest effect on the average elastic modulus, but stress localization and strength, for examples, could be greatly affected by local variation of the yarn geometry [3,4]. The level of detail required in the description of the yarn geometry to accurately capture the effect of the architecture is still an open question.

Idealized yarn geometry have been proposed by many authors to construct geometric models of woven fabrics, see e.g. [2,5-7]. Yarns are modeled as solid volumes which bound the fiber bundle. Yarn cross section is often described by simple geometric entities as ellipse or lenticular section. Moreover, it is generally supposed to remain constant along the length of the yarn. Such modeling assumptions may be questionable with respect to the true shape of the yarns cross section in actual material. Constant cross section also often lead to yarn intersections in all but the very simplest weaves. Intersections may be corrected by adjusting the yarn width and rotations at the crossover points in the weave [6], but it would eventually leads to some loss in yarn volume. Yarns interpenetrations could also be tackled by solving an intermediate FE problem using a “separate and compress” approach [2]. It requires, however, the experimental identification of the effective behavior of yarns under compaction. An alternative way to approach the geometry of textile reinforcement is to

explicitly simulate the manufacturing process of these structures [8-10]. The step-by-step simulation of the whole weaving process requires large computational resources. Thus, Miao *et al.* [11] proposed a static relaxation approach which proved to give similar results to an explicit simulation of the weaving process, but for only a fraction of the computational cost. An initial guess fabric structure is constructed with correct topology based upon the fabric weave pattern ; then, a pre-tensile force is applied to the yarns in order to imitate the tension they experience during the weaving process. The fabric deforms until reaching a new equilibrium state which should correspond to the relaxed state of the fabric at the end of the weaving process. This relaxation approach has also be used in [12,13]. It should be noted that a similar approach has also been proposed by Durville based on his previous work on the mechanical behavior of entangled materials [14]: starting from an arbitrary configuration, where yarns interpenetrate each other, tows are moved gradually until their arrangement fulfills the chosen weaving pattern and there is no more interpenetration [15,16].

This paper proposes a simulation procedure based on a relaxation approach to generate realistic geometric models for interlock woven fabrics. An initial fabric geometry is constructed using an idealized solid yarn description. Then, yarns are then discretized into fibers. Tensile forces are imposed to the yarns and are progressively relaxed as the fabric deforms. The mechanical equilibrium is solved using an explicit first-order scheme. Algorithmic aspects are discussed, as well as the effects of the initial geometry and yarn discretization. Finally, a first validation of the developed approach is proposed for a multilayer interlock woven fabric.

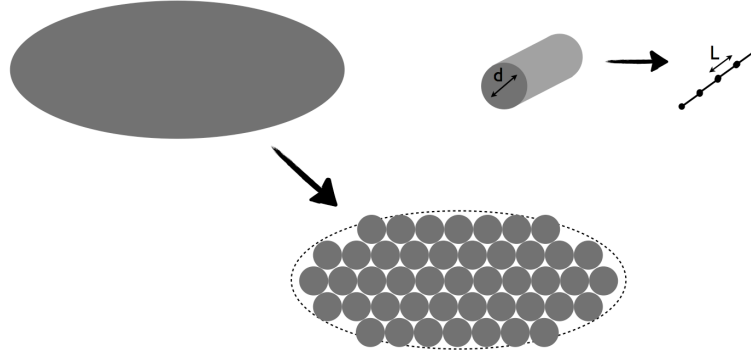


Fig.1. Illustration of the discretization of a yarn into macro-fibers, and macro-fibers into truss elements.

2 Initial fabric geometry

2.1 Idealized geometric model

The initial fabric geometry is constructed using an idealized yarn description as previously proposed by the authors [7]. The relative arrangement of the yarns is deduced from the weaving pattern of the fabric. The topology of the fabric is conveniently described by a matrix coding of the warp paths. The yarns are approximated as solid volumes with constant elliptic cross-section. Their center line is calculated by minimizing the yarn bending energy in each crimp elementary interval, i.e. interval between two supporting yarns. An example of a resulting idealized geometry is depicted in Fig. 2.

2.2 Yarn discretization

Following the concept of “digital chain” previously introduced by Wang *et al.* [8], each yarn is decomposed into an assembly of macro-fibers. The number of macro-fibers used to represent a yarn is far smaller than the actual amount of real fibers contained in a yarn. It is assumed that each macro-fiber represents a bundle of real fibers. Macro-fibers are further divided into frictionless pin-connected truss elements along their length (cf. Fig. 1). Only tensile deformation in their axial direction is considered, and it is assumed that no deformation exists in the macro-fiber transverse direction. The macro-fibers are initially densely packed inside the yarn cross-section. The truss element length L is chosen to be the same order than the diameter d of the corresponding macro-fiber.

3 Relaxation algorithm

To simulate the tension the yarns experience during the weaving process, an external force f_e is imposed to the each truss element as:

$$f_e = -E.A.\alpha \quad (1)$$

where E is the Young modulus of the fibers, A their cross section area, and α is a load parameter. The reaction force of a truss element is simply given by:

$$f_i = E.A.\frac{L-L_0}{L_0} \quad (2)$$

where L_0 is its initial length, and L its current length. The applied load f_e will force the macro-fibers to shrink and cause the yarns to straighten. The macro-fibers will eventually enter into contact and rearrange themselves, modifying the initial shape of the yarns. The applied load is gradually relaxed as the truss elements are deformed, until a mechanical equilibrium is reached when

$$\sum f_e = \sum f_i \quad (3)$$

3.1 Contact handling

Contact between macro-fibers is detected using the NBS algorithm [18] which proved to give an optimal linear contact detection time. When a contact is

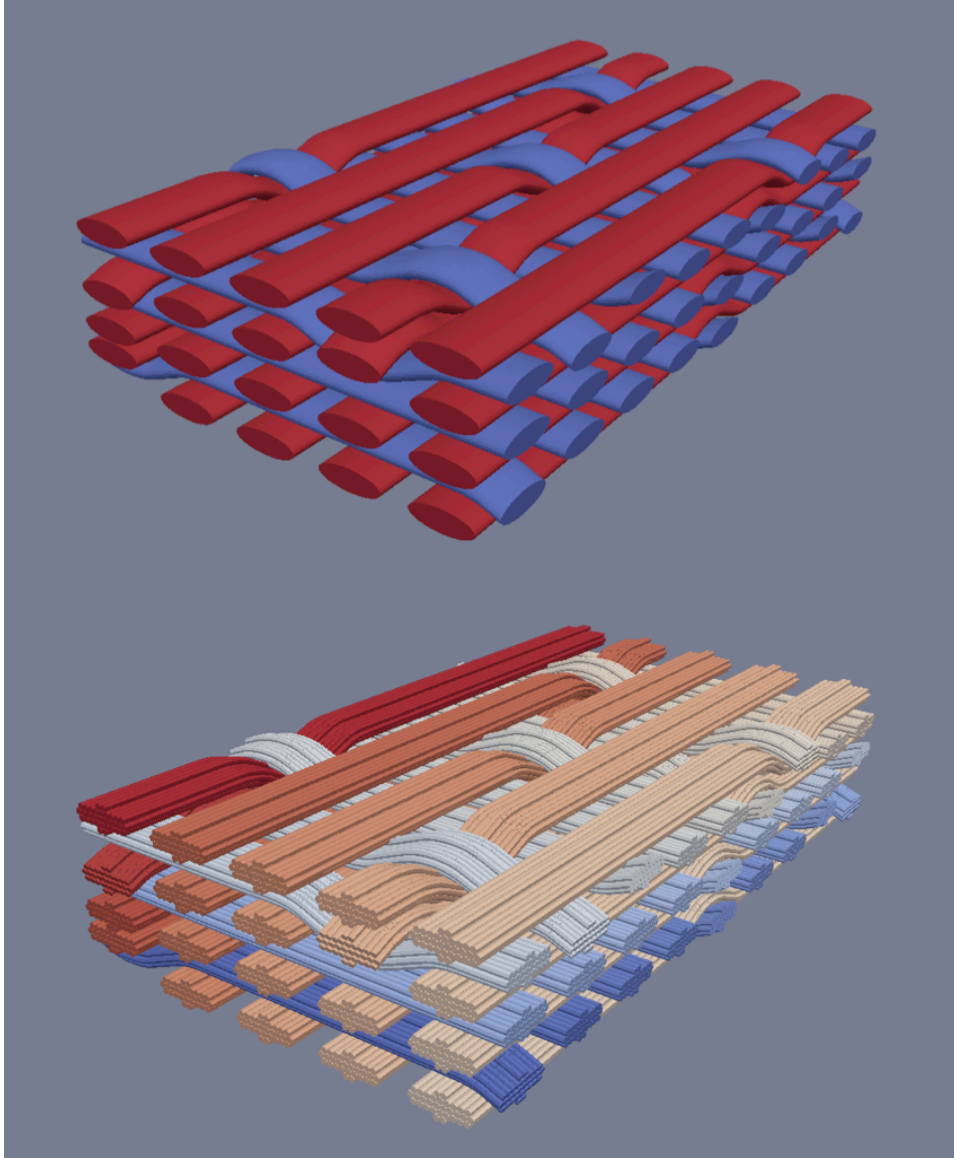


Fig.2. Idealized woven fabric geometric model (top) and corresponding initial discretized model with 32 macro-fibers per yarn (bottom)

detected, i.e. when the distance between two truss elements is smaller than the diameter of the corresponding macro-fibers, contact elements are introduced between the nodes of the interpenetrated truss elements. Contact element constitutive law has the form of a penalty law linking the normal reaction f_c to the penetration depth δ

$$f_c = K(\delta) \cdot \delta \quad (4)$$

where $K(\delta)$ is the normal stiffness of the contact element. K is initially set equal to $p \cdot E$, where p is a penalty coefficient. For very small penetration however, the penalty coefficient is adjusted using a quadratic regularization law [15] in order to stabilize the contact algorithm and avoid spurious oscillations during the relaxation process. Only normal contact is considered, i.e. no friction is taken into account. Contact detection is performed at every step of the relaxation process. Upon separation of two

contacting macro-fibers, the existing contact elements are removed.

4.2 Boundary conditions

Truss nodes of the warp (resp. weft) ends are only allowed to move in the yz -plane (resp. xz -plane), i.e. the x - and y - dimensions of the unit cell remain fixed. Boundary conditions could be imposed on each end of individual macro-fibers, or only in a weak manner by prescribing the displacement of the barycenter of the yarn ends [16]. In addition, when the fabric exhibit a periodic weaving pattern, periodic conditions could be prescribed on the x - and y -boundaries of the unit cell.

The preform could also be compacted in the z -direction by the means of two rigid moving tools to ensure the final thickness of the relaxed fabric. Contact detection between the compacting plates and the macro-fibers is performed by checking the z -coordinates of their corresponding truss element nodes. The non-penetration condition is ensured by imposing the same penalty law than for the contact between macro-fibers.

4.3 Numerical resolution

The mechanical equilibrium is solved iteratively using an in-house explicit dynamic finite element algorithm implemented in ANSYS C. Compared to the original static relaxation approach [11] or the Durville's method [14-16] that utilize an implicit static solver, using an explicit dynamic relaxation

procedure greatly minimizes computer memory resource since it doesn't require to assemble any stiffness matrix.

A first-order central difference scheme is employed:

$$\begin{aligned} \sum (f_e + f_i + f_c)_k &= m \cdot (a_k - \zeta \cdot v_k) \\ v_{k+\frac{1}{2}} &= v_{k-\frac{1}{2}} + a_k \cdot \Delta t \\ u_{k+1} &= u_k + v_{k+\frac{1}{2}} \cdot \Delta t \end{aligned} \quad (5)$$

where m is the mass of a truss element, a , v , and u are respectively the acceleration, speed and position of the truss nodes, Δt a the pseudo time step. A viscous parameter ζ is introduced to dampen the high frequency oscillations and to ensure a quasi-static solution. The time step is chosen as a small fraction (typically < 0.05) of the critical time step given by the CFL condition to guarantee the convergence of the algorithm.

5 Numerical analysis and verification

5.1 Effect of the relaxation parameters

Besides the physical properties of the fibers, i.e. their Young's modulus E and their density ρ , the relaxation process is mainly governed by the load parameter α (Eq. 1) and the damping parameter ζ (Eq. 5). In this work, we focus on the relaxed geometry of the fabric, and not on quantifying the mechanics of the weaving process. Therefore, the

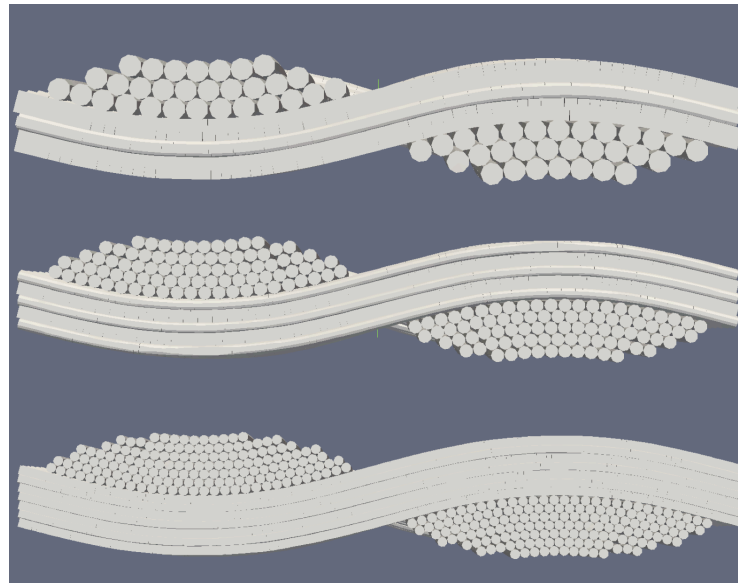


Fig.3. Comparison of the final relaxed geometry for a plain weave fabric with an increasing number of macro-fiber per yarns, respectively 33, 86 and 157 from top to bottom.

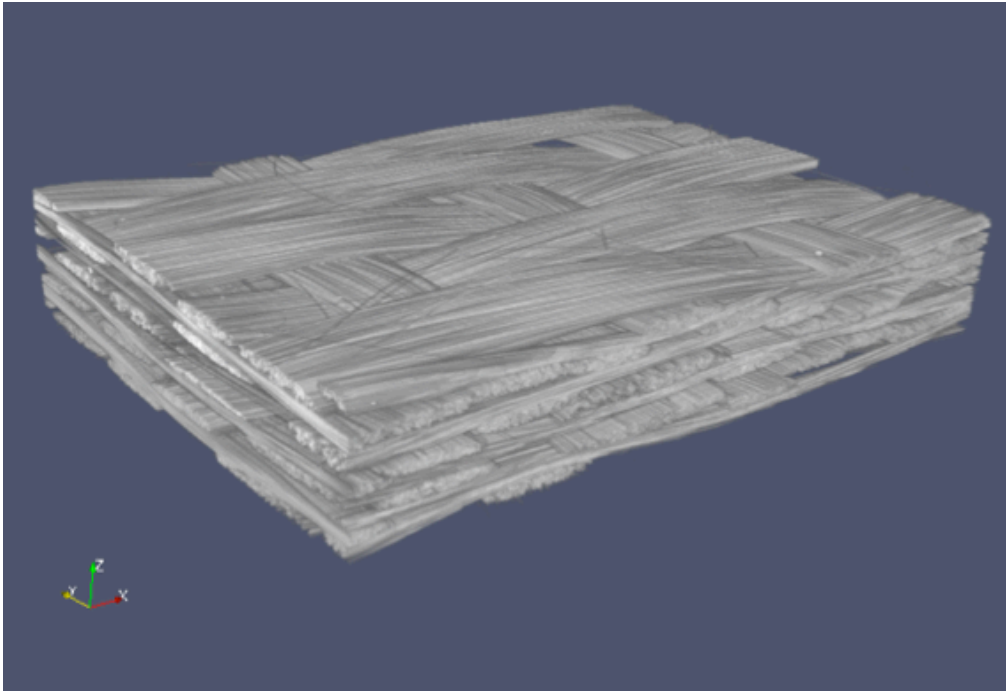


Fig.4 X-ray CT of the woven fabric used for the validation of the relaxation procedure

load parameter α could be chosen artificially larger than the actual load applied to the fabric in order to speed-up the relaxation process. It was checked that, for the same targeted thickness, final geometry

remains consistent for different values of α . The only difference is that a lower α value would require more iterations to converge. However, α should not be chosen too large as, when α is increased, ζ should

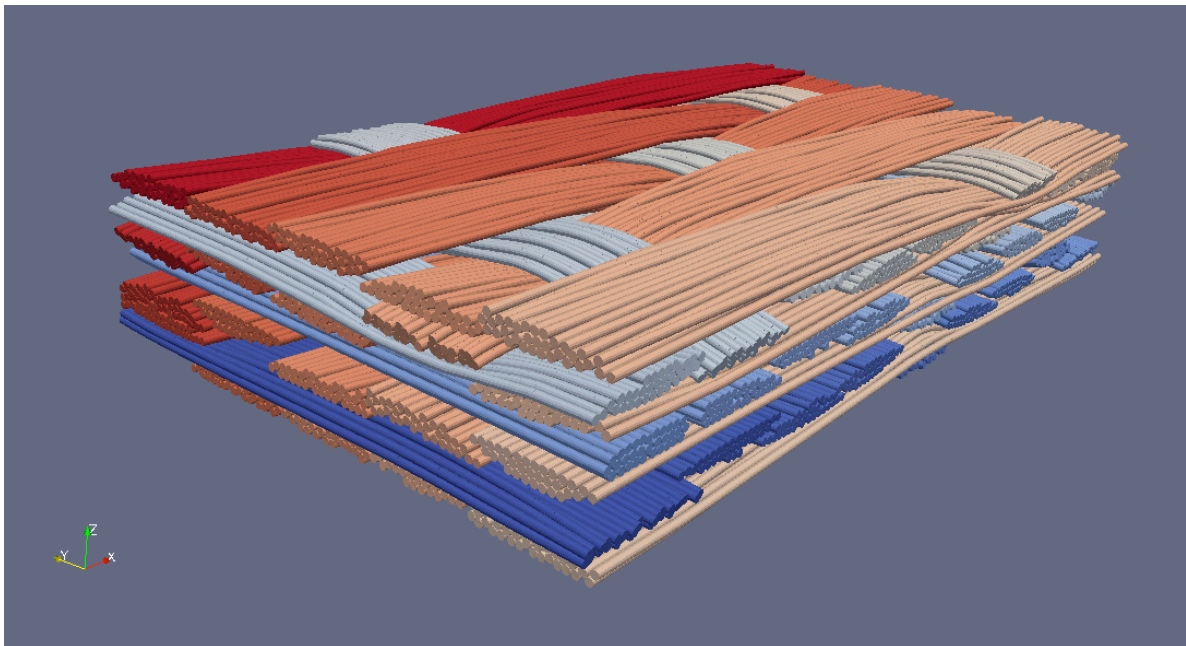


Fig.5 Discretized model after relaxation and compaction to a thickness of 1.5 mm.

be increased accordingly to ensure that the solution remains quasi-static. In the meantime, the time step should be diminished to guarantee convergence, thus increasing the number of iterations. In the following, α is typically chosen between 5 and 10, and ζ around 1.5, which were empirically found to be the optimal values for our calculations.

5.2 Effect of the initial conditions

The effect of the initial shape of the yarns and the number of macro-fibers per yarn on the relaxed geometry of the fabric have been studied for a plain weave and a multilayer twill fabric. Relaxation results show that the number of macro-fibers used to discretize the yarns cross section barely affect the final shape of the yarn (cf. Fig. 3), as long as it is sufficient to describe the topology of the yarn cross section. Similar results were already mentioned by Miao *et al* [11] who stated that 19 macro-fibers per yarns provide sufficient accuracy for 3D braided fabric. The same observations can be made concerning the effect of the initial shape of the yarns: the same final shape is obtained either by starting from a circle or an elliptic yarn cross section for example. However, it is advantageous to choose an initial cross section close to the expected final shape of the yarn: the number of iteration required to attain the requested thickness is reduce in a large extent.

6 Validation

The relaxation procedure has been applied to a real multilayer interlock woven. X-ray computed tomography (CT) data of the studied preform were

obtained while the fabric being compacted to a thickness of 1.5 mm (Fig. 4). The corresponding initial idealized geometric model is depicted in Fig. 2 alongside the initial discretized model. Due to the inherent restrictions of the idealized geometric approach, the initial model could not have a thickness inferior to 1.8 mm to avoid yarn interpenetration. Thus, the thickness of the idealized model was initially set to 2 mm. The area of the yarn cross section was chosen so that it corresponds to the final fiber volume fraction in the actual fabric.

The modeled unit cell contains 20 warp yarns and 27 weft yarns. Each yarn is discretized into 32 macro-fibers, i.e. a total of 1405 macro-fibers and approximately 450,000 truss elements. The discretized model was compacted and relaxed using the method described in Section 3. Best result was found by applying first a low external load ($\alpha=1$) without compaction for a moderate number of iterations (<1000). This pre-relaxation step would correct any initial small interpenetration which would have occurred during the discretization process. Then, a larger external load ($\alpha=7$) is applied with compaction being active; the rigid compacting plates are displaced gradually while keeping the external load constant. A slow compaction speed was chosen to keep the relaxation process quasi-static. Once the targeted thickness was attained ($t=1.5\text{mm}$), a small number of post-relaxation steps was performed. The whole relaxation/compaction process required 150,000 iterations and a total CPU time of 5 hours using a 3GHz Intel Core2 Q9650 single core.

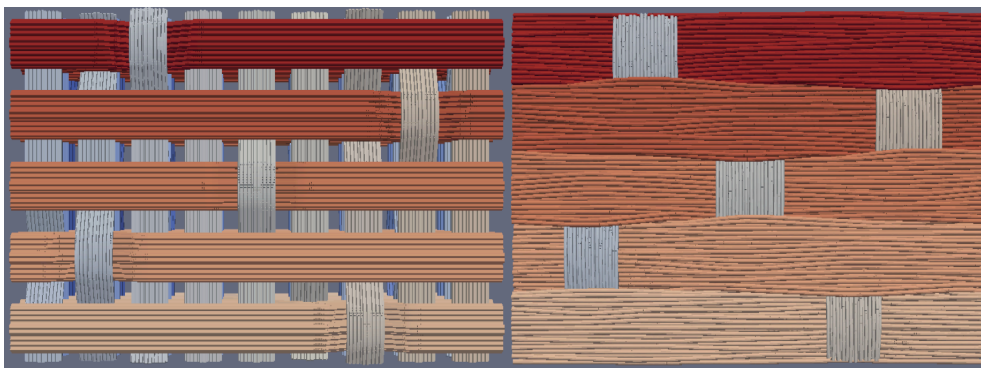


Fig.6. Discretized model before (left) and after (right) relaxation and compaction. Top view.

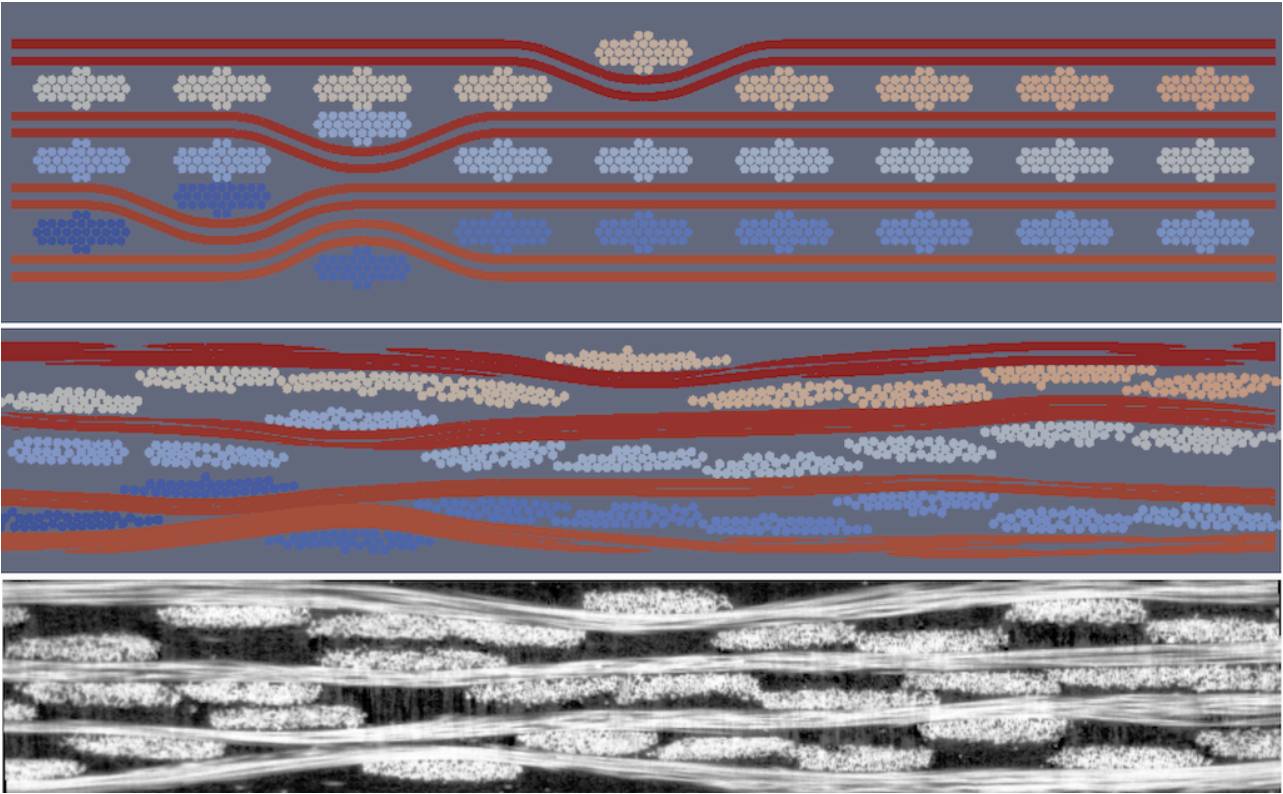


Fig.7. Discretized model before (top) and after (middle) relaxation and compaction, and corresponding slice from the X-ray tomography of the real fabric (bottom). Side view normal to weft direction.

The resulting model is shown in Fig. 5. It is visually close to the actual fabric. There is an evident improvement over the idealized geometry when compared with the initial model shown in Fig. 2. The effect of the relaxation and compaction process is illustrated in Fig. 6. Clearly, the yarns spread as the fabric is compacted. After compaction, outer surfaces of the model don't exhibit porosity anymore, which is consistent with observations on the real fabric. The model is also able to reproduce the variation of the cross section of the yarns along the length of the unit cell.

A qualitative comparison of the initial and relaxed discretized models and the actual fabric is given in Fig. 7. The locations and shape of the porosity compare favorably with the X-ray CT data. The relative position of the yarns is also in good agreement, even if small differences could still be observed. Some deviations could be explained by the fact that the relaxation process starts from an idealized model which doesn't include the geometric variability of the actual fabric (e.g. deviation of the yarn paths from the weft or warp direction, or misalignment of weft columns) Still, the main features of the fabric architecture, like crimp angles or contacting yarns, are well reproduced by the relaxed model. A first comparison between yarns

shape and size of both the final discretized model and the X-ray CT data was performed by manually fitting ellipses to yarns cross sections on corresponding slices. The cross section areas compare favorably with a maximum relative difference of 1.5%. A deviation inferior to 10% was observed for the length of the ellipses axes. Yarns in the relaxed model tend to be a little larger (and thinner) than in the real material. These measurements, however, could be influenced by the manual contouring process, and a more systematic procedure is being developed based on active contour models [19].

7 Conclusion

We proposed a numerical procedure to generate realistic geometric models of woven fabrics. It is based on the representation of yarns as bundle of fibers. The final model is obtained through a relaxation process of an initial idealized geometric model, and takes into account the contact interaction between fibers. The developed approach was applied to the simulation of a multilayer interlock woven fabric. Preliminary results demonstrate this approach is able to capture the main features of a real woven architecture with only very few numerical parameters. Even if some small discrepancies could

still be observed, the final relaxed model is visually close to the real material, and represents a major improvement when compared to the initial idealized geometric model.

Current work focuses on validating the relaxation approach on various woven and braided preforms. More quantitative comparisons of yarns paths and cross section will be carried out using dedicated morphological analysis tools [20]. The geometric variability of the real material will be addressed through the incorporation of suitable statistical models. Finally, this approach would be eventually integrated into our virtual material modeling toolbox for ceramic matrix composites [17].

Acknowledgments

This work was supported by Herakles, Safran Group.

References

- [1] A. Mouritz, M. Bannister, P. Falzon and K. Leong “Review of applications for advanced three-dimensional fibre textile composites”. *Compos. Part A*, Vol. 30, pp 1445–1461, 1999.
- [2] Lomov et al. “Meso-FE modeling of textile composites: road map, data flows and algorithms”. *Compos. Sci. Technol.*, Vol. 67, pp 1870-1891, 2007.
- [3] B. Cox and G. Flanagan, *Handbook of analytical methods for textile composites*, Contractor Report 4750, NASA, 1997.
- [4] S. Kari, M. Kumar, I. Jones, N. Warrior, and A. Long, Effect of yarn cross-sectional shapes and crimp on the mechanical properties of 3d woven composites, in Proceedings of the 17th International Conference on Composite Materials, 2008.
- [5] S. Lomov, A. Gusakov, G. Huysmans, A. Prodromou and I. Verpoest “Textile geometry preprocessor for meso-mechanical models of woven composites”. *Compos. Sci. Technol.*, Vol. 60, pp 2083-2095, 2000.
- [6] M. Sherburn, *Geometrical and mechanical modeling of textiles*, PhD thesis, University of Nottingham, 2007.
- [7] G. Couégnat, E. Martin and J. Lamon “Multiscale modeling of the mechanical behavior of woven composite materials”. *Proceedings of the 17th International Conference on Composite Materials (ICCM17)*, Edinburgh, UK, 2009.
- [8] Y. Wang and X. Sun “Digital element simulation of textile processes”. *Compos. Sci. Technol.*, Vol. 64, pp 311-319, 2001.
- [9] H. Finckh, “Numerische Simulation der mechanischen Eigenschaften textiler Flächengebilde Gewebeherstellung (Numerical simulation of the mechanical properties of textile fabrics)”, in *Proceedings of the German 3rd LS-DYNA Forum*, 2004.
- [10] A. Pickett, J. Sirtautas, and A. Erber, “Braiding Simulation and Prediction of Mechanical Properties”, *Appl. Compos. Mater.*, Vol. 16, pp. 345–364, 2009.
- [11] Y. Miao, E. Zhou, Y. Wang and B. Cheeseman “Mechanics of textile composites: micro-geometry”. *Compos. Sci. Technol.*, Vol. 68, pp 1671-1678, 2008
- [12] E. Zhou, D. Mollenhauer, and E. Iarve, A realistic 3-d textile geometric model. *Proceedings of the 17th International Conference on Composite Materials*, Edinburgh, UK, 2009.
- [13] Y. Mahadik and S. Hallett, “Finite element modelling of tow geometry in 3D woven fabrics”, *Compos. Part A*, Vol. 41, pp 1192-1200, 2010.
- [14] D. Durville, Numerical simulation of entangled materials mechanical properties, *Journal of Materials Science*, 40 (2005), pp. 5941–5948.
- [15] D. Durville, “A finite element approach of the behaviour of woven materials at microscopic scale”, in *Mechanics of Microstructured Solids*, J.-F. Ganghoffer and F. Pastrone, eds., vol. 46 of Lecture Notes in Applied and Computational Mechanics, Springer, 2009, pp. 39–46.
- [16] D. Durville “Simulation of the mechanical behavior of woven fabrics at the scale of fibers”. *Int. J. Mater. Form.*, Vol. 3, pp 1241-1251, 2010.
- [17] G. Couégnat, W. Ros, T. Haurat, C. Germain, E. Martin and G. Vignoles “An integrated virtual material approach to ceramic matrix composites”. *Proceedings of the 36th International Conference on Advanced Ceramics and Composites (ICACC)*, Daytona Beach, USA, 2012.
- [18] A. Munjiza and K. Andrews “NBS contact detection algorithm for bodies of similar size”. *Int. J. Numer. Meth. Engng*, Vol. 43, pp 131-149, 1998.
- [19] M. Kass, A. Witkin, and D. Terzopoulos, “Snakes: Active contour models”, *Int. J. Comput. Vision*, 1, pp. 321–331, 1988.
- [20] C. Chapoulié, J.-P. Da Costa, C. Germain, M. Cataldi and G. Vignoles. “Multiscale extraction of morphological features in woven CMC”, *Proceedings of the 37th International Conference on Advanced Ceramics and Composites (ICACC)*, Daytona Beach, USA, 2013.